New Porous Lanthanide-Organic Frameworks: Synthesis, Characterization, and Properties of Lanthanide 2,6-Naphthalenedicarboxylates

Xiangjun Zheng,[a] Changyan Sun,[a] Shaozhe Lu,[b] Fuhui Liao,[c] Song Gao,[c] and Linpei Jin*[a]

Keywords: Carboxylate ligands / Coordination polymers / Hydrothermal synthesis / Lanthanides / X-ray diffraction

Three porous, 3-D coordination polymers $[Pr_4(NDC)_6(H_2O)_6]\cdot 2H_2O$ (**1**), $[Eu_4(NDC)_6(H_2O)_5]\cdot 3H_2O$ (**2**) and $[Yb_2(NDC)_3(H_2O)]\cdot H_2O$ (**3**) based on lanthanide 2,6-naphthalenedicarboxylates (NDC) were synthesized by hydrothermal reactions of lanthanide chlorides with NDC and their properties were investigated. Polymers **1**, **2** and **3** differ in the coordination environment of the Ln^{III} ions. Their 3-D networks are reminiscent of the shape of a compressed honeycomb, showing 1-D open channels. The guest water molecules and coordinating water molecules are enclathrated in the channels. The photophysical properties of the Eu^{3+} complex were investigated by high-resolution luminescence spectroscopy. The results indicate that there are four Eu^{III} ion sites in complex **2**, which is in accordance with the results of the single-crystal X-ray diffraction studies. Thermogravimetric and variable-temperature powder X-ray diffraction analyses show that the porous frameworks of this series of complexes are relatively stable. The framework remained even when the guest molecules were lost and did not collapse until the temperature reached 430 °C. The magnetic properties of **2** were also investigated.

Introduction

The assembly of porous networks has been an intriguing field for their potential applications in catalysis,[1,2] adsorption and separation processes,[3−9] ion exchange,[10,11] and sensor technology.[12,13] Many molecular-based porous materials constructed by coordination polymers have been reported.[6−9,14−17] These open-framework coordination polymers possess unprecedented pore size, shape and function. However, the main problem encountered in designing such coordination polymers is the interpenetration of networks or collapse of the framework upon removal of the guest molecules enclathrated in the cavities.[9] The modification of the ligand and the selection of the metal ions are the key points to avoid the interpenetration of networks. Thus far, porous coordination polymers have centered on the assembly of carboxylates and d-block metal ions such as Zn^{II},[9] Cu^{II},[14] and Co^{II} [17,18] as d-block metal ions have low coordination numbers and the coordination sites of d-block metal ions are easily occupied by the carboxylates, therefore interpenetration of the framework is less likely to occur. Lanthanide ions have higher coordination numbers, and it is more difficult to predict or control the coordination frameworks of lanthanide ions than their d-block analogues. The interpenetration of frameworks can frequently be seen in lanthanide coordination polymers because many coordination sites are accessible for the bridging ligand. However, incorporation of ancillary ligands (such as water molecules) into lanthanide coordination networks is also more feasible, and these ancillary ligands can occupy some coordination sites and prevent the frameworks from interpenetrating. At the same time, they may be removed without collapse of the lanthanide-organic framework, thereby generating porous solids with coordinatively unsaturated and Lewis-acidic lanthanide ions that have potential catalytic activity.[19,20] Additionally, the inherent flexibility of their coordination geometry is particularly attractive for the preparation of new network types as this greater structural ambivalence will lead to the synthesis of unprecedented structures. Based on the fact that lanthanide ions have a high affinity for oxygen-containing ligands, we selected a rigid linear ligand, 2,6-naphthalenedicarboxylate, to construct lanthanide coordination polymers. In the present case, we report the synthesis and structure of lanthanide naphthalenedicarboxylates; their properties were inves-

[a] Department of Chemistry, Beijing Normal University, Beijing 100875, People's Republic of China
Fax: +86-10-6220-2075
E-mail: lpjin@bnu.edu.cn
[b] Laboratory of Excited States Processes, Chinese Academy of Sciences; Changchun Institute of Optics, Fine Mechanics and Physics, Chinese Academy of Sciences, Changchun 130021, People's Republic of China
[c] State Key Laboratory of Rare Earth Materials Chemistry and Applications, PKU-HKU Joint Laboratory on Rare Earth Materials and Bioinorganic Chemistry, College of Chemistry, Peking University, Beijing 100871, People's Republic of China

  DOI: 10.1002/ejic.200400176

tigated systematically. They are porous and quite thermally stable because they have channels with incorporated solvents, which may be removed without the collapse of the framework.

Results and Discussion

Syntheses and Structures

Dipotassium 2,6-naphthalenedicarboxylate easily forms a precipitate upon the addition of lanthanide chloride, therefore in the preparation of the coordination polymers, the 2,6-naphthalenedicarboxylate was acidified first to facilitate the growth of crystals. 1,10-Phenanthroline (phen), which is a mild organic base, was also added to promote the hydrothermal reaction. Klinowski et al. have reported the crystal structure of $[Yb_2(NDC)_3(H_2O)]\cdot 2H_2O$ from the reaction of $YbCl_3\cdot 6H_2O$, 2,6-naphthalenedicarboxylic acid and triethylamine.[21] The difference between $[Yb_2(NDC)_3(H_2O)]\cdot 2H_2O$ and complex **3** is a lattice water molecule, which cannot have a significant effect on the crystal structure. Therefore, only the structures of complexes **1** and **2** will be discussed here.

There are four crystallographically independent Ln^{III} cations and six NDC anions in the unit cells of **1** and **2**, while for **3** there are only two Yb^{III} ions and three NDC anions in the asymmetric unit. In **1**, **2** and **3**, the Ln^{III} ions are all coordinated to oxygen atoms, with Ln−O distances in the range 2.357(9)−2.745(12) Å for **1**, 2.302(16)−2.625(15) Å for **2** and 2.169(9)−2.323(19) Å for **3**, characteristic of the lanthanide contraction. The NDC ligand adopts a bis(bidentate bridging) coordination mode where every NDC ligand bridges four Ln^{III} cations.

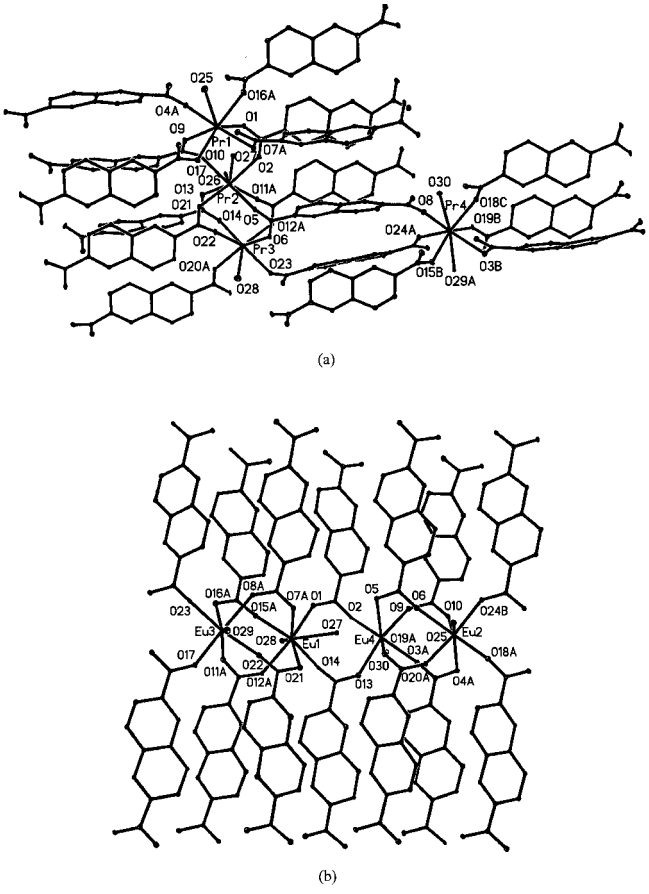

Figure 1. Coordination environment of **1** (a) and **2** (b); lattice water molecules and all hydrogen atoms have been omitted for clarity; thermal ellipsoids are shown at 10% probability

There are four Pr^{III} ions, six NDC anions, six coordinated water molecules and two lattice water molecules in the asymmetric unit of **1**. Pr1 and Pr3 are both sevenfold coordinated, with six oxygen atoms from six NDC ligands and one oxygen atom from a water molecule, while Pr2 and Pr4 are both eightfold coordinated, with six oxygen atoms from six NDC ligands and two oxygen atoms from two water molecules [see (a) in Figure 1]. Pr1 and Pr2 are connected by two μ_2-carboxylates from two NDC ligands. Pr2 and Pr3 are connected by four μ_2-carboxylates from four NDC ligands; Pr4 is connected to Pr2 and Pr3 through the bridging of two NDC ligands. The Pr^{3+} ions along the *a*-axis are bridged together, resulting in an infinite zigzag chain with the order Pr3···Pr2···Pr1···Pr4A···Pr3A···, with Pr···Pr distances of 4.133(2), 4.196(2), 4.131(2) and 5.001(2) Å, respectively. The chains may be viewed as secondary building blocks that are further cross-linked by the $C_{10}H_4$ spacers of the NDC anions. when viewed along the *a*-axis, the resulting 3-D network of **1** is reminiscent of the shape of a compressed honeycomb, showing 1-D open channels (Figure 2). The guest water molecules and coordinated water molecules are enclathrated in the channels.

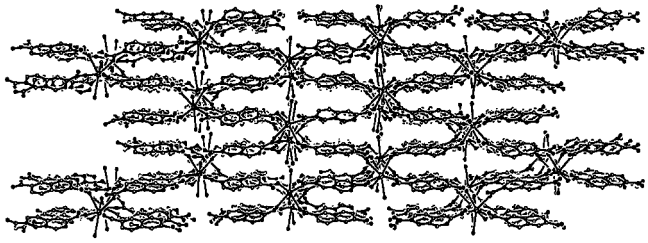

Figure 2. 3-D open-framework of **1** containing 1-D channels viewed along the *a*-axis; all hydrogen atoms and lattice water molecules have been omitted for clarity

There are four Eu^{III} ions, six NDC anions, five coordinated water molecules and three lattice water molecules in the asymmetric unit of **2**. Eu2, Eu3 and Eu4 have a sevencoordinate environment [see (b) in Figure 1] like Pr1 and Pr3 in **1**, while Eu1 is located in an eight-coordinate environment like Pr2 and Pr4 in **1**. Eu1 and Eu3 are connected by four μ_2-carboxylates from four NDC ligands. This is also the case for Eu2 and Eu4; Eu1 and Eu4 are linked by two μ_2-carboxylates from two NDC ligands. The Eu^{3+} ions along the *a*-axis are arranged in the order Eu3···Eu1···Eu4···Eu2···Eu3A···, with Eu···Eu distances of 4.997(2), 4.073(2), 4.805(2) and 4.064(2) Å, respectively. When viewed along the *a*-axis, this complex exhibits the same porous honeycomb-like architecture as **1**. Removing all hydrogen atoms, the coordinated and guest water mol-

ecules from the crystal structure of **2** gives the ball-and-stick model and the space-filling model shown in Figure 3. The ball-and-stick model shows a quite large opening in the cross section of the open channel, but the space-filling model shows that only the middle part of this is an effective cavity, with dimensions of about 5.0 × 2.1 Å^2.

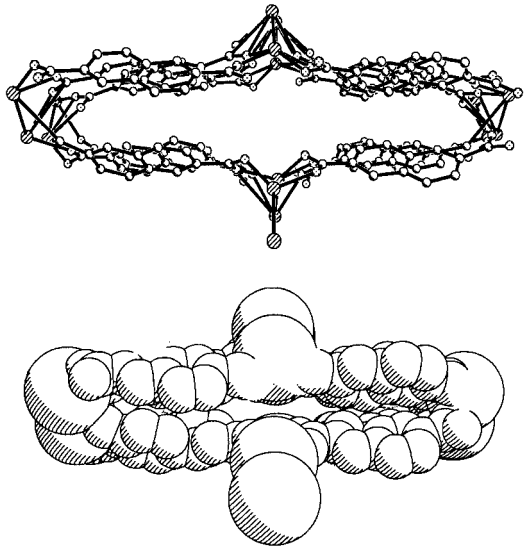

Figure 3. Cross-section of the open channel in **2** (all hydrogen atoms and water molecules have been omitted): ball-and-stick model (top), space-filling model (bottom)

These results show that **1**, **2** and **3** are different in the coordination environment of Ln^{III} ions, but they nevertheless form similar 3-D porous coordination polymers with the same topology. The sizes of the pores are also similar. When viewed along the *b*-axis, the coordination polymers of **1**, **2** and **3** can exhibit 3-D inorganic-organic hybrid architectures (Figure 4). The inorganic sheets are composed of Ln^{3+} ions, and the organic sheets are composed of NDC ligands; the two sheets alternate. The adjacent sheets are linked together through $Ln-O_{COO^-}$ coordination bonds.

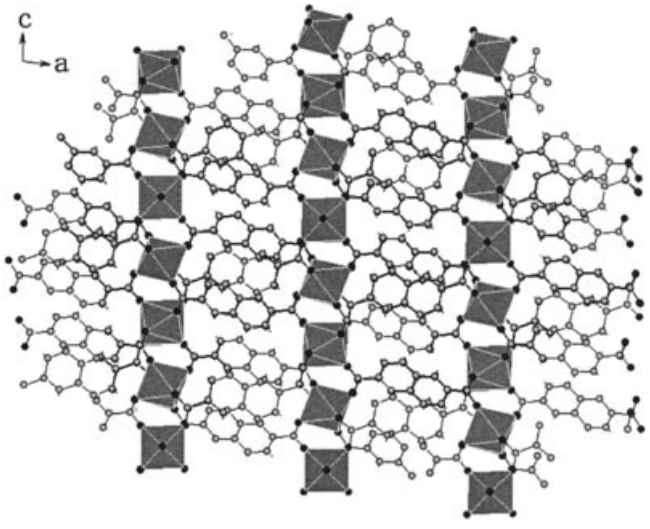

Figure 4. The inorganic-organic hybrid structure of **2**

Photophysical Properties of 2

The Eu^{III} ion is frequently used as a structural probe to investigate local symmetry.[22] The lowest emission level, $^5D_0$, and the ground state, $^7F_0$, are both nondegenerate, therefore the number of excitation peaks corresponding to the $^7F_0 \rightarrow {}^5D_0$ transition will reveal the number of Eu^{3+} ions with different coordination environments in the compound. The high-resolution emission spectrum of **2** corresponding to $^5D_0 \rightarrow {}^7F_J$ (J = 0−4) transitions excited at a wavelength of 355 nm at 77 K is shown in Figure 5. The most intense transition is $^5D_0 \rightarrow {}^7F_2$, which implies red emission light of **2**. No obvious and direct information about the Eu^{3+} ion sites can be obtained from Figure 5, but from the time-resolved spectra (Figure 6) corresponding to $^5D_0 \rightarrow {}^7F_J$ (J = 1, 2) transitions, it can be seen that both the shape and number of the emission peaks change. It can be concluded that there is more than one Eu^{3+} ion site in **2**. Selective excitation techniques were applied to further probe the number of Eu^{3+} ion sites in **2**. With 16107 and 16232 cm^{-1} as the monitoring wavenumbers, and scanning in the range 17280−17229.5 cm^{-1} ($^7F_0 \rightarrow {}^5D_0$), the excitation spectra shown in Figure 7 (a and b) were obtained. There are obviously three groups of peaks located at 17260.7, 17255.4 and 17249.1 cm^{-1}, respectively. Although a broadened $^7F_0 \rightarrow {}^5D_0$ excitation band is often seen in europium coordination polymers, it is worthy of note that there is a shoulder at the peak located at 17253.3 cm^{-1}. The average Eu−O bond lengths for Eu1, Eu2, Eu3 and Eu4 are 2.412, 2.372, 2.372 and 2.391 Å, respectively. However, around Eu2 there is a lattice water molecule, O26, and the distance between Eu2 and O26 [2.80(2) Å] suggests a weak coordination interaction, making the coordination bonds around Eu2 more ionic than those around Eu3. The longer a bond is, the more ionic character the bond possesses and the higher the energy needed to excite the europium ion. Therefore the four peaks at 17260.7, 17255.4, 17253.3 and 17249.1 cm^{-1} in Figure 7a can be ascribed to the $^5D_0$ levels of Eu1, Eu4, Eu2 and Eu3, respectively, confirming that

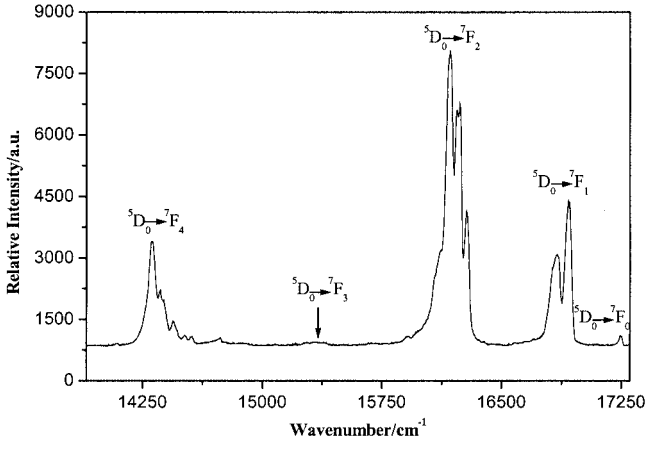

Figure 5. Emission spectrum of **2** corresponding to $^5D_0 \rightarrow {}^7F_J$ (J = 0 ~ 4) transitions at 77 K (λ_{exc} = 355 nm)

four Eu^{3+} ion sites exist in **2**, which is in agreement with the X-ray diffraction results.

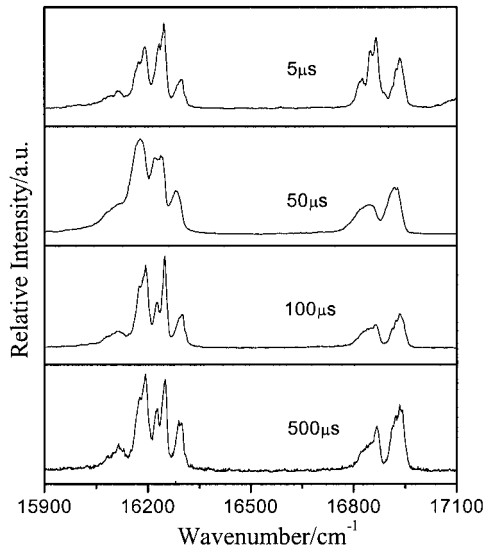

Figure 6. Time-resolved spectra of **2** at 77 K in the range 17100−15900 cm^{-1}; delay time: 5 μs, 50 μs, 100 μs and 500 μs; λ_{exc} = 355 nm

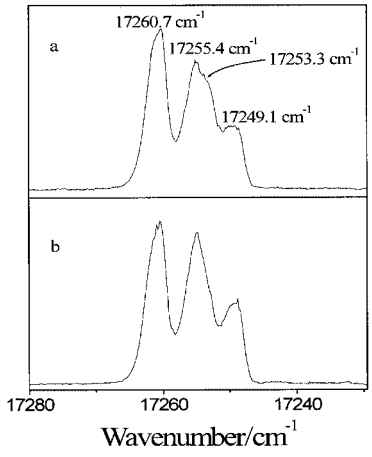

Figure 7. Excitation spectra of **2**; analyzing wavenumbers: a 16107 cm^{-1}; b 16232 cm^{-1}

Thermal Stability Analysis of 2

TG analysis of **2** is consistent with the crystallographic observations. The first weight loss of 5.06% from 103 °C to 186 °C (Figure 8) corresponds to the loss of three lattice water molecules and three coordinated water molecules (calculated: 5.31%), leaving a framework of $[Eu_4(NDC)_6 \cdot 2H_2O]$. Between 271 °C and 308 °C, the sample undergoes a second weight loss of 1.31%. During this process the two coordinated water molecules that have a stronger interaction with the Eu^{3+} ions [Eu1−O28: 2.474(15) Å; Eu2−O25: 2.451(15) Å] and are also involved in hydrogen bonding with carboxylate oxygen atoms [O25···O14 ($-x + 1/2$, $y + 1/2$, $-z + 1/2$) 2.758 Å; O28···O18 ($-x + 3/2$, $y - 1/2$, $-z + 1/2$) 2.844 Å] are removed (calculated: 1.77%), leaving a framework of $[Eu_4(NDC)_6]$. $[Eu_4(NDC)_6]$ remains stable up to 430 °C at which temperature it begins to decompose.

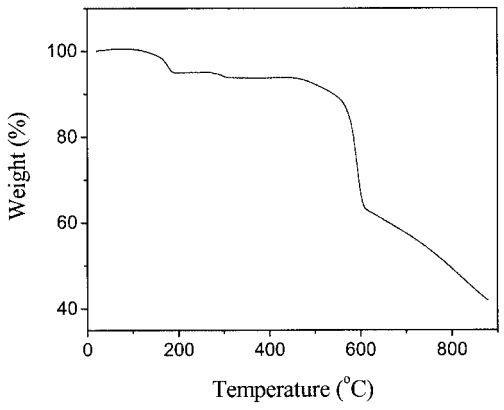

Figure 8. TG curve of **2**

To further test the thermal stability of **2**, powder samples were examined by powder X-ray diffraction analysis. Corresponding to the TG analysis, powder XRD patterns (Figure 9) were recorded at 27, 200, 250, 300, 350, 400, 450, 500 and 700 °C. It can be seen from Figure 9 that the XRD pattern at 200 °C is different from that at room temperature. The major peaks shift a little to higher 2θ value, indicating that a distortion of the structure has occurred, although this does not affect the existence of the framework. From 200 °C to 400 °C the major peaks in the XRD patterns at five different temperatures show no change in their position, indicating that the framework is able to survive the heat treatment and is thermally stable despite the removal of the water molecules. Above 450 °C the XRD pattern changes significantly, revealing the collapse of the framework, which is in accordance with the result of thermogravimetric analysis.

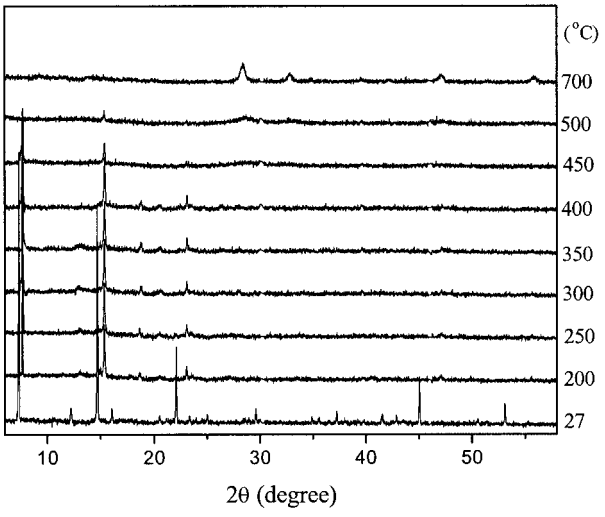

Figure 9. Powder X-ray diffraction patterns of **2** at different temperatures

The results of thermogravimetric analyses for **1** and **3** show a similar stability to **2**.

Magnetic Properties of 2

The variable temperature magnetic susceptibility of **2** was measured in the range 2−304 K. The plot of $\chi_M T$ vs. T is shown in Figure 10, where χ_M is the corrected molar magnetic susceptibility per $[Eu]_4$ unit. The observed $\chi_M T$ at room temperature is 5.0 $cm^3 \cdot mol^{-1} \cdot K$, less than the value 6.0 for four Eu^{III} ions calculated from the van Vleck equation allowing for population of the lower excited state of ^7F_J (Eu^{3+}) in **2** at 293 K. As the temperature is lowered, $\chi_M T$ decreases continuously due to the depopulation of the Stark levels for a single Eu^{III} ion. At the lowest temperature, $\chi_M T$ is close to zero, indicating a $J = 0$ ground state of the Eu^{III} ion ($^7F_0$). The magnetic susceptibility above 150 K follows the Curie−Weiss law due to the presence of thermally populated excited states.

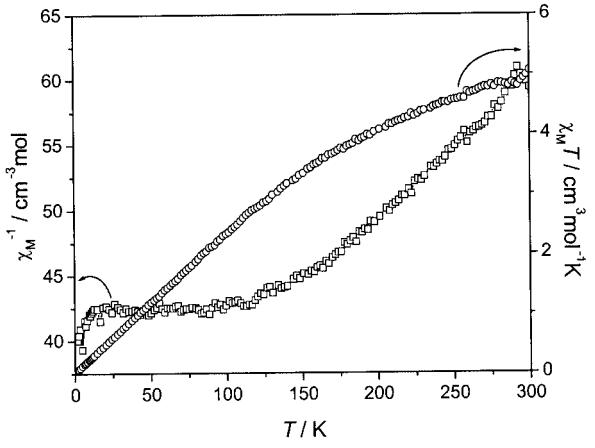

Figure 10. Plot of the temperature dependence of $\chi_M T$ (O) and χ_M^{-1} (□) for the title complex (per $[Eu]_4$unit)

Experimental Section

General: $PrCl_3 \cdot 6H_2O$, $EuCl_3 \cdot 6H_2O$ and $YbCl_3 \cdot 6H_2O$ were prepared by dissolving their oxides in concentrated hydrochloric acid and then evaporating the solvents dryness. All the other reagents are commercially available and were used without further purification. Elemental analyses were obtained on an Elementar Vario EL analyzer. The IR spectra were recorded with a Nicolet Avatar 360 FT-IR spectrometer using the KBr pellet technique. Thermogravimetric analyses were performed with a TGA: 951 Thermogravimetric Analyzer. The magnetic susceptibilities were obtained on a crystalline sample using an Oxford MagLab System 2000 magnetometer. The experimental susceptibilities were corrected for the sample holder and the diamagnetism contributions estimated from Pascal's constants. The powder X-ray diffraction patterns were recorded on a Bruker AXS D8 ADVANCE diffractometer.

$[Pr_4(NDC)_6(H_2O)_6] \cdot 2H_2O$ (1): Two drops of hydrochloric acid (1.65 $mol \cdot L^{-1}$) were added to a mixture of dipotassium 2,6-naphthalenedicarboxylate (0.044 g, 0.15 mmol) and H_2O (3 mL) and the mixture was stirred. $PrCl_3 \cdot 6H_2O$ (0.036 g, 0.1 mmol) and phen·H_2O (0.02 g, 0.1 mmol) were then added. The mixture was sealed in a 25 mL stainless steel reactor with Teflon liner and heated at 200 °C for 72 h. Green crystals of **1** were obtained in 76.3% yield (0.038 g). $C_{72}H_{52}O_{32}Pr_4$ (1992.8): calcd. C 43.40, H 2.63; found C 43.86, H 2.61. IR data (KBr pellet): $\tilde{\nu}$ = 3446 s, 2970 m, 1602 m, 1542 s, 1408 s, 1352 s, 1196 m, 924 m, 797 m, 560 m, 493 m cm^{-1}.

$[Eu_4(NDC)_6(H_2O)_5] \cdot 3H_2O$ (2): Two drops of hydrochloric acid (1.65 $mol \cdot L^{-1}$) were added to a mixture of dipotassium 2,6-naphthalenedicarboxylate (0.044 g, 0.15 mmol) and H_2O (3 mL) and the mixture was stirred. $EuCl_3 \cdot 6H_2O$ (0.037 g, 0.1 mmol) and phen·H_2O (0.04 g, 0.2 mmol) were then added. The mixture was sealed in a 25 mL stainless steel reactor with Teflon liner and heated at 200 °C for 72 h. Light-yellow crystals of **2** were obtained in 78.4% yield (0.04 g). $C_{72}H_{52}Eu_4O_{32}$ (2037.0): calcd. C 42.45, H 2.57; found C 42.99, H 2.24. IR data (KBr pellet): $\tilde{\nu}$ = 3508 m, 1602 m, 1547 s, 1491 s, 1412 s, 1353 s, 1199 m, 927 m, 795 s, 564 m, 492 m cm^{-1}.

$[Yb_2(NDC)_3(H_2O)] \cdot H_2O$ (3): Two drops of hydrochloric acid (1.65 $mol \cdot L^{-1}$) were added to a mixture of dipotassium 2,6-naphthalene-

Table 1. Crystal data for complexes **1**, **2** and **3**

Compound	**1**	**2**	**3**
Empirical formula	$C_{72}H_{52}O_{32}Pr_4$	$C_{72}H_{52}Eu_4O_{32}$	$C_{36}H_{22}O_{14}Yb_2$
Molecular mass	1992.78	2036.98	1024.62
Temperature (K)	293(2)	293(2)	293(2)
Wavelength (Å)	0.71073	0.71073	0.71073
Crystal system	monoclinic	monoclinic	monoclinic
Space group	$P2_1/c$	$P2_1/n$	$C2/c$
a (Å)	17.295(7)	17.006(6)	23.183(9)
b (Å)	15.194(7)	15.130(5)	8.344(4)
c (Å)	26.334(9)	24.973(8)	17.558(8)
α (°)	90	90	90
β (°)	112.35(2)	106.361(6)	98.568(9)
γ (°)	90	90	90
V (Å^3)	6400(4)	6165(3)	3359(3)
Z	4	4	4
D_c [g·cm^{-3}]	2.068	2.194	2.026
μ (mm^{-1})	3.094	4.120	5.607
Reflections collected, unique, R_{int}	26941, 11624, 0.1245	20778, 8866, 0.1549	7617, 2958, 0.0877
R_{int} [$I > 2\sigma(I)$]	R_1 = 0.0493, wR_2 = 0.0588	R_1 = 0.0607, wR_2 = 0.1056	R_1 = 0.0527, wR_2 = 0.1001

Table 2. Selected bond lengths (Å) and bond angles (°) for complexes **1**, **2** and **3**[a]

1		**2**		**3**	
Pr(1)−O(1)	2.414(7)	Eu(1)−O(14)	2.309(15)	Yb(1)−O(1)	2.169(9)
Pr(1)−O(4)$^{\#1}$	2.419(7)	Eu(1)−O(15)$^{\#10}$	2.313(15)	Yb(1)−O(1)$^{\#16}$	2.169(9)
Pr(1)−O(17)	2.443(8)	Eu(1)−O(7)$^{\#11}$	2.369(16)	Yb(1)−O(3)$^{\#17}$	2.247(11)
Pr(1)−O(7)$^{\#2}$	2.445(8)	Eu(1)−O(1)	2.371(17)	Yb(1)−O(3)$^{\#18}$	2.247(11)
Pr(1)−O(9)	2.452(9)	Eu(1)−O(21)	2.374(17)	Yb(1)−O(5)	2.316(10)
Pr(1)−O(16)$^{\#3}$	2.528(10)	Eu(1)−O(12)$^{\#12}$	2.462(14)	Yb(1)−O(5)$^{\#16}$	2.316(10)
Pr(1)−O(25)	2.636(11)	Eu(1)−O(28)	2.474(15)	Yb(1)−O(7)	2.323(19)
Pr(2)−O(10)	2.400(8)	Eu(1)−O(27)	2.625(15)	Yb(2)−O(6)$^{\#19}$	2.187(10)
Pr(2)−O(11)$^{\#4}$	2.433(7)	Eu(2)−O(24)$^{\#13}$	2.302(16)	Yb(2)−O(6)	2.187(10)
Pr(2)−O(2)	2.435(9)	Eu(2)−O(18)$^{\#13}$	2.335(16)	Yb(2)−O(4)$^{\#20}$	2.206(10)
Pr(2)−O(21)	2.452(8)	Eu(2)−O(4)$^{\#14}$	2.347(15)	Yb(2)−O(4)$^{\#18}$	2.206(10)
Pr(2)−O(5)	2.467(9)	Eu(2)−O(10)	2.383(15)	Yb(2)−O(2)	2.229(10)
Pr(2)−O(13)	2.540(8)	Eu(2)−O(6)	2.388(16)	Yb(2)−O(2)$^{\#19}$	2.229(10)
Pr(2)−O(27)	2.545(8)	Eu(2)−O(20)$^{\#15}$	2.400(14)		
Pr(2)−O(26)	2.714(8)	Eu(2)−O(25)	2.451(14)		
Pr(3)−O(23)	2.403(7)	Eu(3)−O(22)	2.307(16)		
Pr(3)−O(20)$^{\#5}$	2.410(10)	Eu(3)−O(23)	2.328(15)		
Pr(3)−O(22)	2.416(7)	Eu(3)−O(16)$^{\#10}$	2.337(17)		
Pr(3)−O(14)	2.452(8)	Eu(3)−O(17)	2.339(16)		
Pr(3)−O(12)$^{\#4}$	2.460(8)	Eu(3)−O(11)$^{\#12}$	2.345(17)		
Pr(3)−O(6)	2.517(9)	Eu(3)−O(8)$^{\#11}$	2.439(16)		
Pr(3)−O(28)	2.604(11)	Eu(3)−O(29)	2.51(2)		
Pr(4)−O(24)$^{\#6}$	2.357(9)	Eu(4)−O(3)$^{\#14}$	2.317(15)		
Pr(4)−O(15)$^{\#7}$	2.431(9)	Eu(4)−O(2)	2.323(15)		
Pr(4)−O(3)$^{\#8}$	2.432(8)	Eu(4)−O(19)$^{\#15}$	2.365(16)		
Pr(4)−O(19)$^{\#9}$	2.441(8)	Eu(4)−O(13)	2.373(18)		
Pr(4)−O(8)	2.481(7)	Eu(4)−O(5)	2.383(15)		
Pr(4)−O(18)$^{\#2}$	2.483(8)	Eu(4)−O(9)	2.439(16)		
Pr(4)−O(30)	2.513(8)	Eu(4)−O(30)	2.537(19)		
Pr(4)−O(29)$^{\#6}$	2.745(12)				

[a] Symmetry operations: $^{\#1}$ $x, -y + 3/2, z + 1/2$; $^{\#2}$ $-x + 1, -y + 2, -z + 1$; $^{\#3}$ $x - 1, -y + 3/2, z - 1/2$; $^{\#4}$ $x, -y + 3/2, z - 1/2$; $^{\#5}$ $-x + 2, -y + 2, -z + 2$; $^{\#6}$ $-x + 2, -y + 2, -z + 1$; $^{\#7}$ $-x + 2, y + 1/2, -z + 3/2$; $^{\#8}$ $-x + 1, y + 1/2, -z + 1/2$; $^{\#9}$ $x, y, z - 1$; $^{\#10}$ $x + 1/2, -y + 1/2, z + 1/2$; $^{\#11}$ $-x + 1, -y + 1, -z + 1$; $^{\#12}$ $x + 1/2, -y + 1/2, z - 1/2$; $^{\#13}$ $x - 1, y, z$; $^{\#14}$ $x - 1/2, -y + 1/2, z - 1/2$; $^{\#15}$ $-x + 1, -y + 1, -z$; $^{\#16}$ $-x + 1, y, -z + 1/2$; $^{\#17}$ $-x + 3/2, y + 1/2, -z + 1/2$; $^{\#18}$ $x - 1/2, y + 1/2, z$; $^{\#19}$ $-x + 1, -y + 1, -z$; $^{\#20}$ $-x + 3/2, -y + 1/2, -z$.

dicarboxylate (0.044 g, 0.15 mmol) and H_2O (15 mL) and the mixture was stirred. $YbCl_3 \cdot 6H_2O$ (0.039 g, 0.1 mmol) was then added. The mixture was sealed in a 50 mL stainless steel reactor with Teflon liner and heated at 180 °C for 72 h. Light-yellow crystals of **3** were obtained in 29.3% yield (0.015 g). $C_{36}H_{22}O_{14}Yb_2$ (1024.6): calcd. C 42.20, H 2.16; found C 42.08, H 2.31. IR data (KBr pellet): $\tilde{\nu}$ = 3447 m, 2977 m, 1693 s, 1602 s, 1574 s, 1423 s, 1293 s, 1193 m, 775 m, 452 m cm^{-1}.

Measurement of the High-Resolution Luminescence Spectra: The excitation light source was a YAG:Nd laser which emits at 1.064 μm, and the excitation wavelength was 355 nm. The sample was placed in a dewar and cooled with liquid nitrogen. The fluorescence data were collected at right angles through a Spex 1403 monochromator with a photomultiplier tube, then averaged with a Boxcar integrator and finally transferred to a computer.

X-ray Crystallographic Study: The X-ray single-crystal data collection for complexes **1**, **2** and **3** was performed on a Bruker Smart 1000 CCD diffractometer, using graphite-monochromated Mo-K_α radiation (λ = 0.71073Å). Semiempirical absorption corrections were applied using the SADABS program. The structures were solved by direct methods and refined by full-matrix least-squares on F^2 using the SHELXTL-97 program.[23] All non-hydrogen atoms were refined with anisotropic displacement parameters. The hydrogen atoms were generated geometrically and treated by a mixture of independent and constrained refinement. Experimental details for X-ray data collection of **1**, **2** and **3** are presented in Table 1, while selected bond lengths for **1**, **2** and **3** are listed in Table 2.

CCDC-228787−228789 (for **1**−**3**) contains the supplementary crystallographic data for this paper. These data can be obtained free of charge at www.ccdc.cam.ac.uk/conts/retrieving.html [or from the Cambridge Crystallographic Data Centre, 12 Union Road, Cambridge CB2 1EZ, UK; Fax: +44-1223-336033; E-mail: deposit@ccdc.cam.ac.uk].

Acknowledgments

This work is supported by National Natural Science Foundation of China (20331010) and State Key Project of Fundamental Research (G1998061308).

[1] J. S. Seo, D.-M. Whang, H.-Y. Lee, S. I. Jun, J.-H. Oh, Y.-J. Jeon, K.-M. Kim, *Nature* **2000**, *404*, 982.
[2] T. Sawaki, Y. Aoyama, *J. Am. Chem. Soc.* **1999**, *121*, 4793.
[3] H. Li, M. Eddaoudi, M. O'keeffe, O. M. Yaghi, *Nature* **1999**, *402*, 276.
[4] S.-I. Noro, S. Kitagawa, M. Kondo, K. Seki, *Angew. Chem. Int. Ed.* **2000**, *39*, 2082.

[5] H. J. Choi, T. S. Lee, M. P. Suh, *Angew. Chem. Int. Ed.* **1999**, *38*, 1405.
[6] M. P. Suh, J. W. Ko, H. J. Choi, *J. Am. Chem. Soc.* **2002**, *124*, 10976.
[7] A. Dimos, D. Tsaousis, A. Michaelides, S. Skoulika, S. Golhen, L. Ouahab, C. Didierjean, A. Aubry, *Chem. Mater.* **2002**, *14*, 2616.
[8] E. J. Cussen, J. B. Claridge, M. J. Rosseinsky, C. J. Kepert, *J. Am. Chem. Soc.* **2002**, *124*, 9574.
[9] M. Eddaoudi, J. Kim, N. Rosi, D. Vodak, J. Wachter, M. O'keeffe, O. M. Yaghi, *Science* **2002**, *295*, 469.
[10] K. S. Min, M. P. Suh, *J. Am. Chem. Soc.* **2000**, *122*, 6834.
[11] O. M. Yaghi, H. Li, *J. Am. Chem. Soc.* **1996**, *118*, 295.
[12] M. Albrecht, M. Lutz, A. L. Spek, G. van Koten, *Nature* **2000**, *406*, 970.
[13] J. A. Real, E. Andrés, M. C. Muñoz, M. Julve, T. Granier, A. Bousseksou, F. Varret, *Science* **1995**, *268*, 265.
[14] J. W. Ko, K. S. Min, M. P. Suh, *Inorg. Chem.* **2002**, *41*, 2151.
[15] L. Pan, K. M. Adams, H. E. Hernandez, X. T. Wang, C. Zheng, Y. Hattori, K. Kaneko, *J. Am. Chem. Soc.* **2003**, *125*, 3062.
[16] Y.-H. Liu, Y.-L. Lu, H.-C. Wu, J.-C. Wang, K.-L. Lu, *Inorg. Chem.* **2002**, *41*, 2592.
[17] P. Ayyappan, O. R. Evans, W. B. Lin, *Inorg. Chem.* **2001**, *40*, 4627.
[18] J. Tao, M.-L. Tong, X.-M. Chen, *J. Chem. Soc., Dalton Trans.* **2000**, 3669.
[19] M. Shibasaki, K.-I. Yamada, N. Yoshikawa, *Lanthanide Lewis Acids Catalysis*, in *Lewis Acids in Organic Synthesis* (Ed.: H. Yamamoto), Wiley-VCH: New York, **1999**; vol. 2.
[20] T. Imamoto, *Lanthanides in Organic Synthesis*; Academic: New York, **1994**.
[21] F. A. A. Paz, J. Klinowski, *Chem. Commun.* **2003**, 1484.
[22] G. R. Choppin, D. R. Peterman, *Coord. Chem. Rev.* **1998**, *174*, 283−299.
[23] G. M. Sheldrick, SHELXTL-97, *Program for the refinement of Crystal Structures*, University of Göttingen, Germany, **1997**.

Received March 3, 2004
Early View Article
Published Online June 11, 2004

